

Supporting Information

pH-Sensitive nanocarrier assisted delivery of adenosine to treat osteoporotic bone loss

Hunter Newman^{1,2‡}, Jiaul Hoque^{2‡}, Yu-Ru V. Shih², Gabrielle Marushack³, Unghyeon Ko², Gavin Gonzales^{2,3}, and Shyni Varghese^{1,2,3*}

¹Department of Mechanical Engineering and Materials Science, Duke University, Durham, NC 27710, USA

²Department of Orthopaedic Surgery, Duke University School of Medicine, Durham, NC 27710, USA

³Department of Biomedical Engineering, Duke University, Durham, NC 27710, USA

‡Authors contributed equally

*To whom correspondence should be addressed. E-mail: shyni.varghese@duke.edu

Synthesis of Cy7 dye conjugated HA-MA-Aln (HA-MA-Aln-Cy7). To prepare the fluorescently labeled polymer, cyanine 7 (Cy7) amine was conjugated to the HA-MA-Aln *via* amide coupling reaction between the free carboxylic acid groups of HA-MA-Aln and the amine group of Cy7. Briefly, HA-MA-Aln (100 mg) was dissolved in a mixture of 1:1 deionized water: DMSO at ~5 mg/mL. To this, EDC.HCl (69 mg) and NHS (41.4 mg) were added at 15 min intervals. After 30 min, Cy7 dissolved in DMSO (6 mg/mL, 1 mL) was added to the reaction mixture, and the reaction was continued for about 48 hours at room temperature. The mixture was dialyzed (using cellulose acetate dialysis membrane, MWCO 3.5 kDa) against 1: 0.1 mixture of DI water: DMSO for 1 day followed by DI water for 4-5 days. The solution was lyophilized and the resulting product, HA-MA-Aln-Cy7, was characterized *via* a combination of UV-visible, and ¹HNMR spectroscopy. The successful conjugation of Cy7 to the HA-MA-Aln backbone was confirmed by UV-visible spectroscopy as the spectra showed typical Cy7 absorption at ~750 nm. The dye content was determined *via* ¹HNMR spectroscopy which showed the presence of aromatic protons (at 7.1-7.3 ppm) from Cy7 and was found to be a conjugation of ~3-4% with respect to the dimeric repeating unit of HA.

Cy7 tagged nanocarrier synthesis and purification. The Cy7 tagged nanocarriers were prepared *via* inverse emulsion photopolymerization using the fluorescently labeled polymers. Briefly, adenosine conjugated 4-OPAm (337.5 mg) was dissolved in DMSO at 150 mg/mL. HA-MA-Aln-Cy7 (37.5 mg, 150 mg/mL) and PEGDA (37.5 mg, 150 mg/mL) were dissolved in 0.5 mL of 0.1M phosphate buffer (pH 7.4). The adenosine conjugated 4-OPAm solution was then added to the solution of HA-MA-Aln-Cy7 and PEGDA, and vortexed. Lithium phenyl-2,4,6-trimethylbenzoylphosphinate (LAP) was separately dissolved in 0.1M phosphate buffer (pH 7.4) at 50 mg/mL and added (0.125 mL) to the mixture. The resulting solution was purged with argon gas and added to a continuous phase consisting of mineral oil with 10% ABIL EM90 surfactant. This mixture was sonicated using a probe sonicator for 90 seconds at 100 W output voltage. Following sonication, the resulting nanoemulsion was UV irradiated for 15 minutes under constant stirring at a speed of 300 rpm. The resulting particles were precipitated using a mixture of 1:1 hexane: isopropanol. The precipitate was centrifuged at 7000 rpm for 10 minutes and washed with 1:1 hexane: isopropanol (4 x 30 mL). The precipitate was washed with pure isopropanol (3 x 30 mL) and suspended in 5 mL DI water (pH ~8.0). The aqueous suspension was immediately flash frozen and freeze-dried to obtain the nanocarriers.

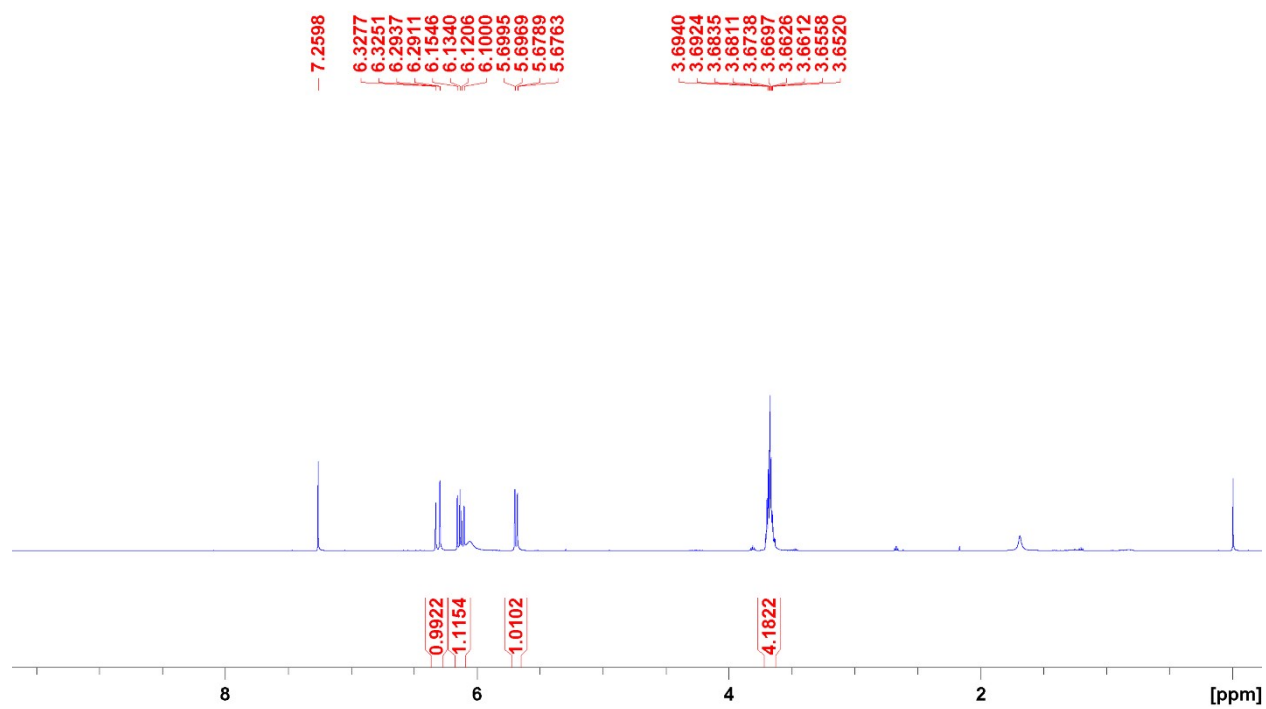


Figure S1. ¹H NMR spectrum of 2-CEAm recorded at 500 MHz in CDCl₃.

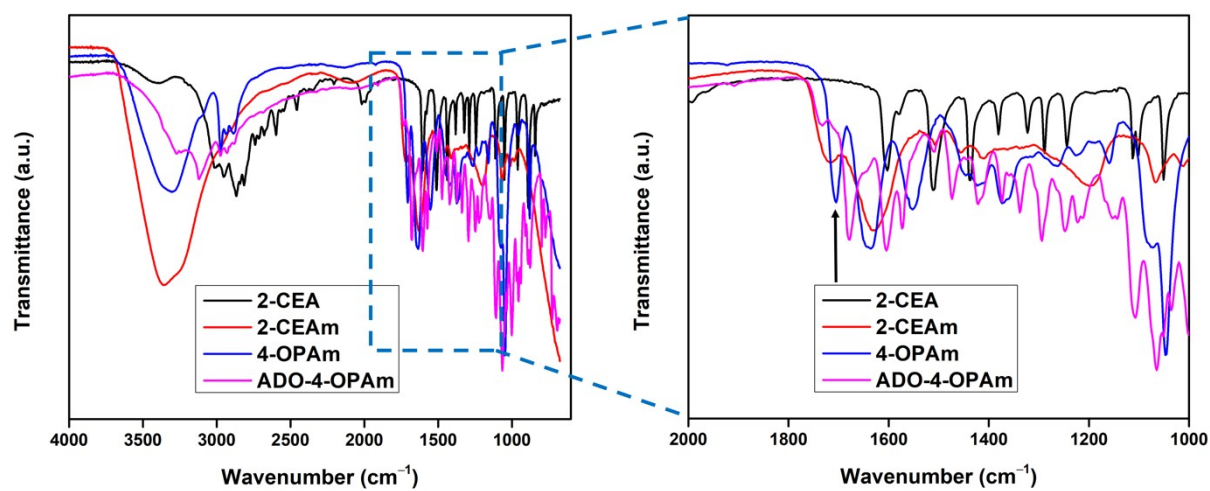


Figure S2. FTIR Spectra of 2-CEA, 2-CEAm, 4-OPAm, and adenosine conjugated 4-OPAm. Full spectrum from 4000-650 cm^{-1} (Left). Extended-spectrum from 2000-1000 cm^{-1} (Right). The arrow at 1705 cm^{-1} in the expanded region shows the presence of C=O stretching frequency of ketone group in 4-OPAm.

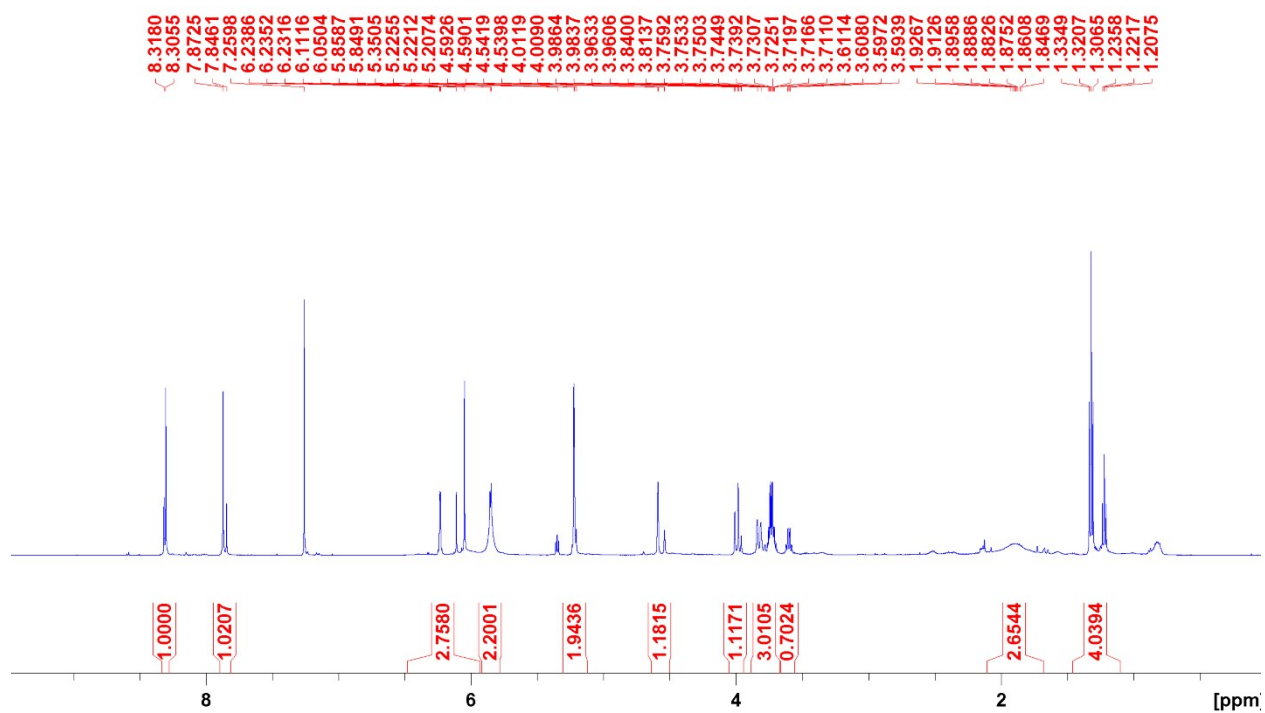


Figure S3. ¹H NMR spectrum of adenosine conjugated 4-OPAm recorded at 500 MHz in CDCl₃.

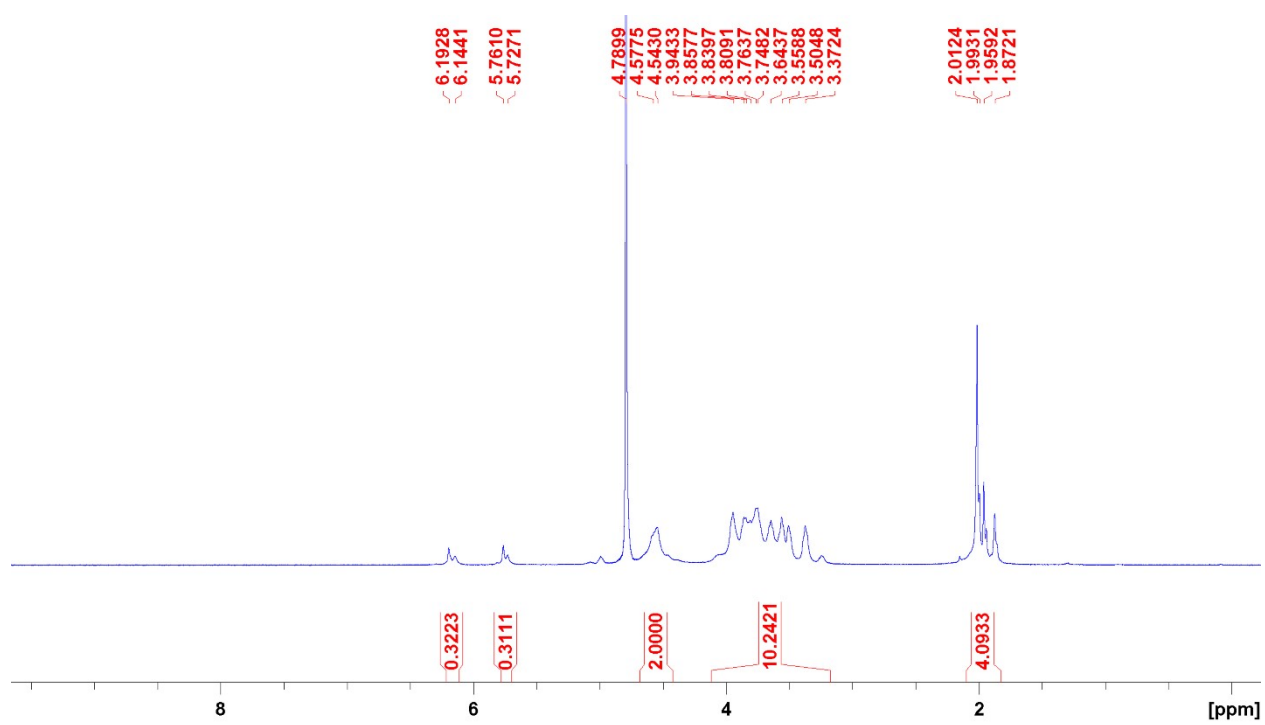


Figure S4. ^1H NMR spectrum of HA-MA recorded at 500 MHz in D_2O .

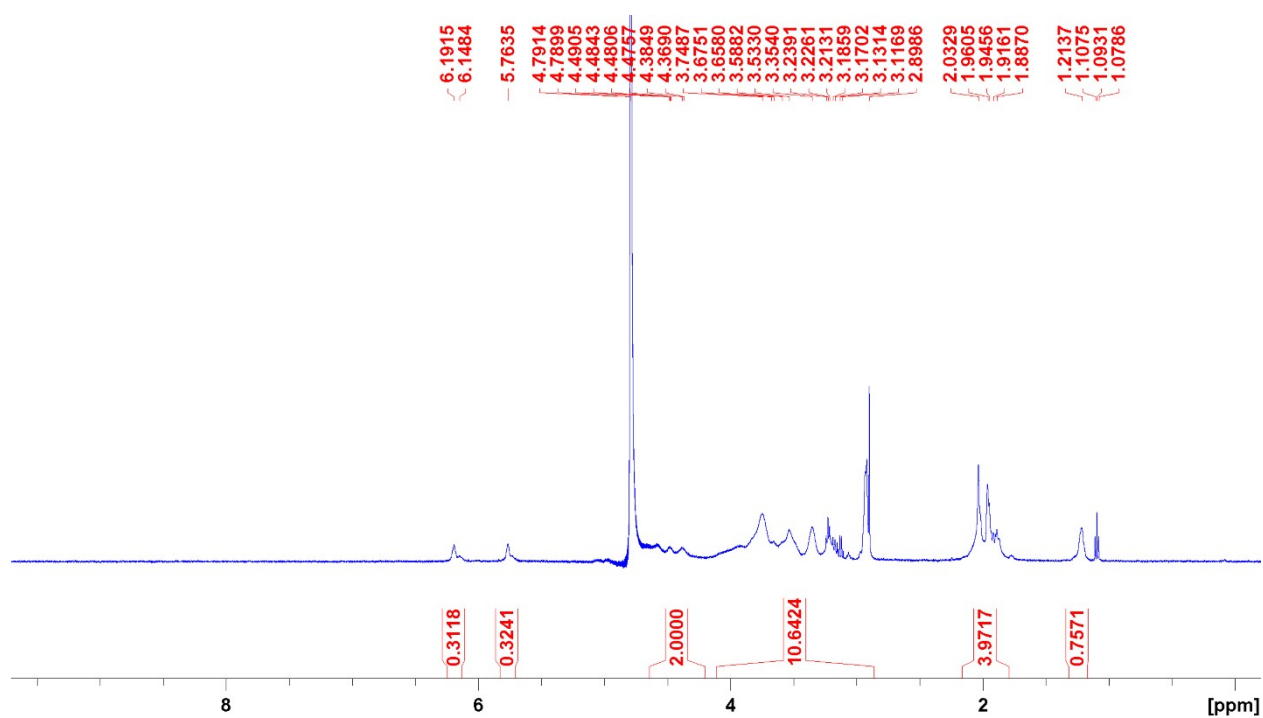


Figure S5. ^1H NMR spectrum of HA-MA-Aln recorded at 500 MHz in D_2O .

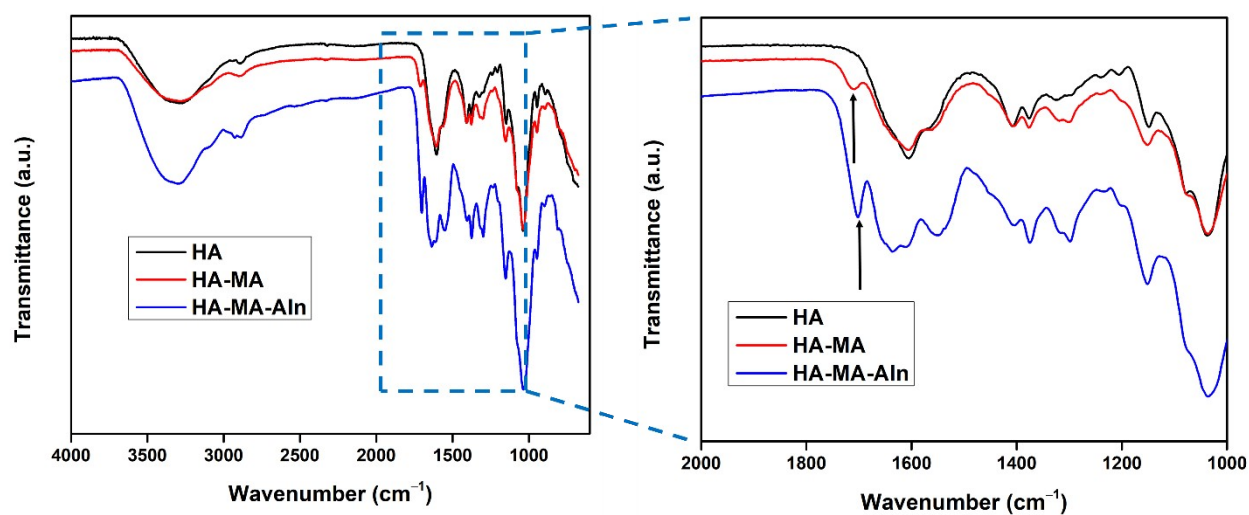


Figure S6. FTIR Spectra of the hyaluronic acid polymers and their derivatives, HA, HA-MA and HA-MA-Aln. Full spectrum from 4000-650 cm^{-1} (Left). Extended-spectrum from 2000-1000 cm^{-1} (Right). Arrow at 1709 cm^{-1} in the expanded region shows the presence of C=O stretching frequency of methacrylate ester group in HA-MA and HA-MA-Aln.

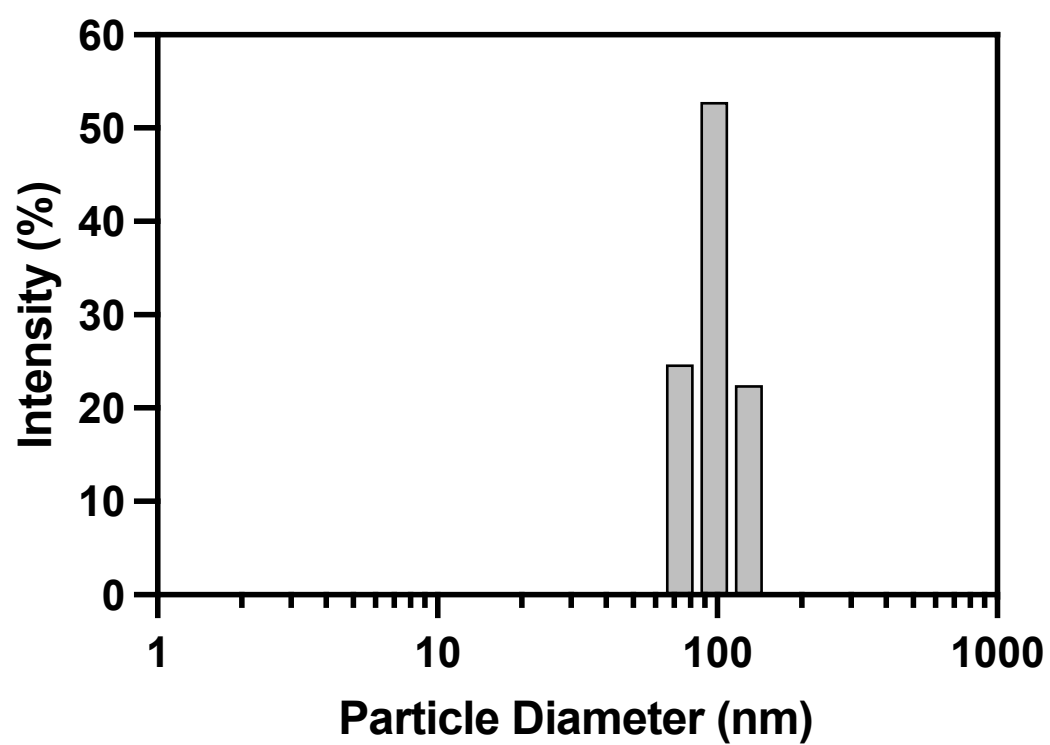


Figure S7. Dynamic light scattering (DLS) particle size distribution of the adenosine-containing nanocarrier (ANC).

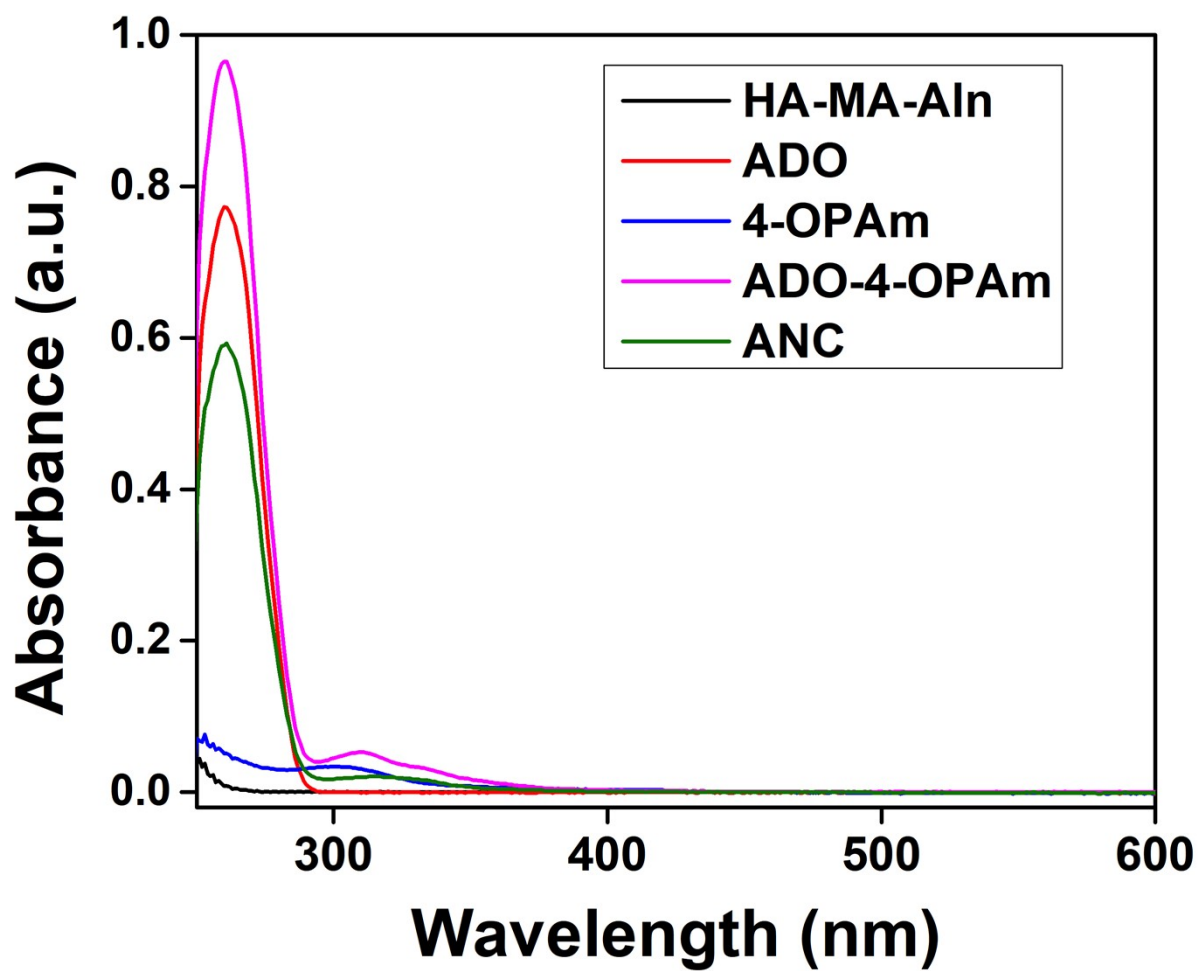


Figure S8. UV-visible absorbance spectra of various reaction products (HA-MA-AIn, adenosine (ADO), 4-OPAm, adenosine conjugated 4-OPAm (ADO-4-OPAm)) and ANC.

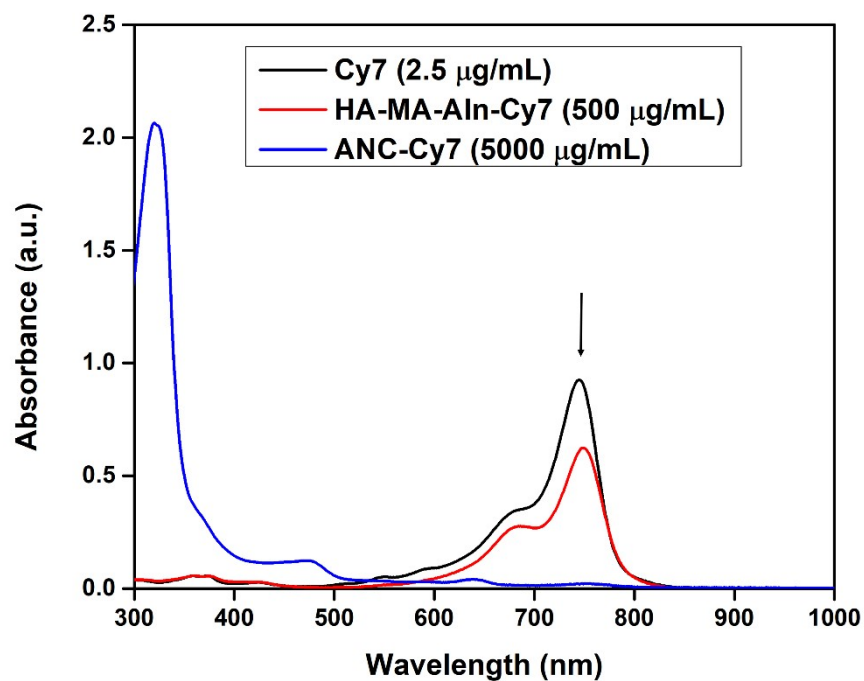


Figure S9. UV-visible absorption spectrum of the cyanine 7.0 labeled nanocarrier (ANC-Cy7). Conjugated cyanine shows similar absorbance as pure cyanine, indicating no structural changes during the reaction and nanocarrier fabrication. Arrow shows absorbance peak for the cyanine 7.0 at ~ 750 nm.

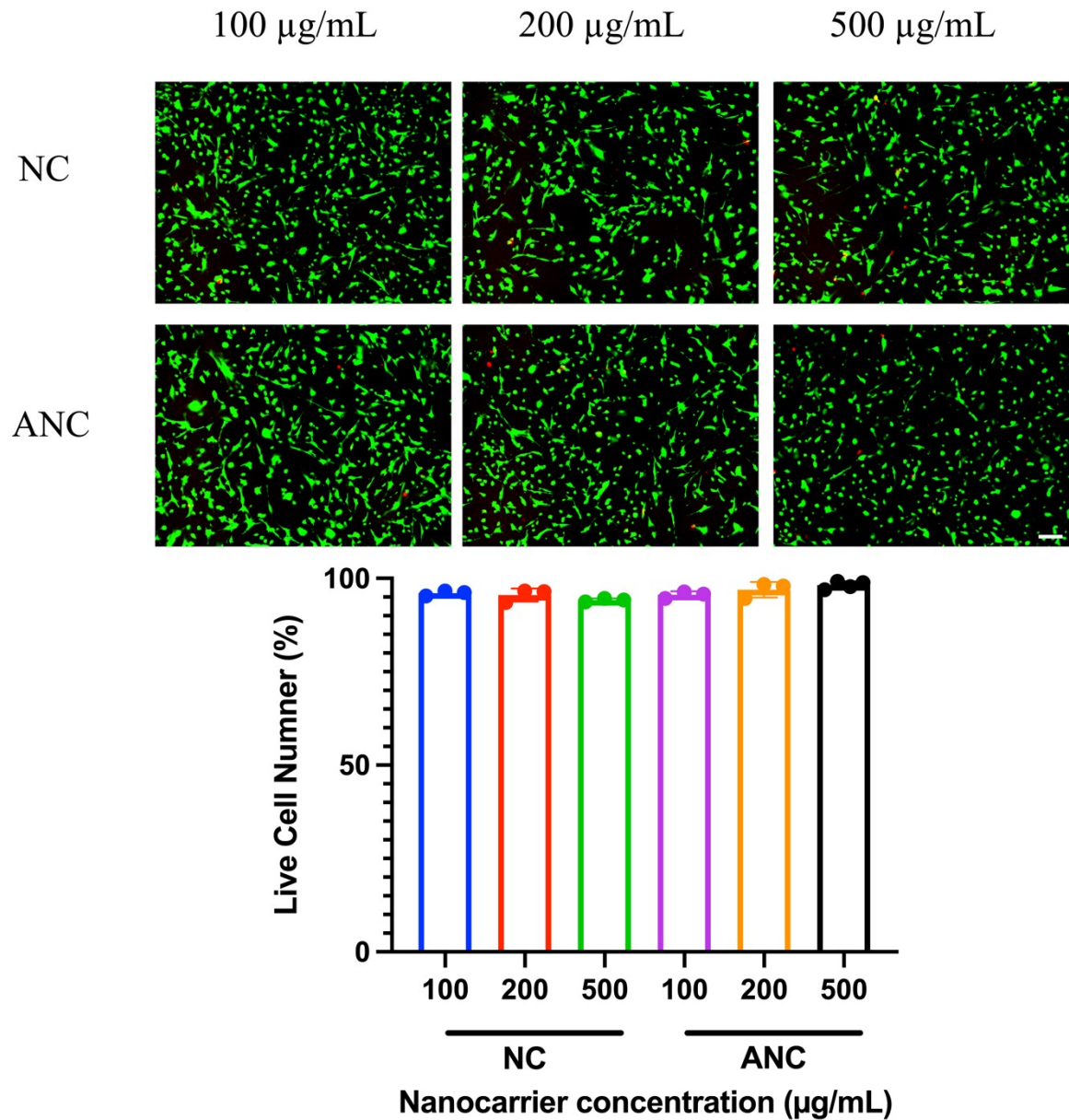


Figure S10. Cytotoxicity of the nanocarriers. (a) Live/dead images of osteoclasts treated with either NC or ANC at various concentrations of 100 $\mu\text{g/mL}$, 200 $\mu\text{g/mL}$, and 500 $\mu\text{g/mL}$ for 24 hours. (b) Quantification of the live/dead images. Green: live cells. Red: dead cells. $n = 3-4$; Scale bar: 50 μm .

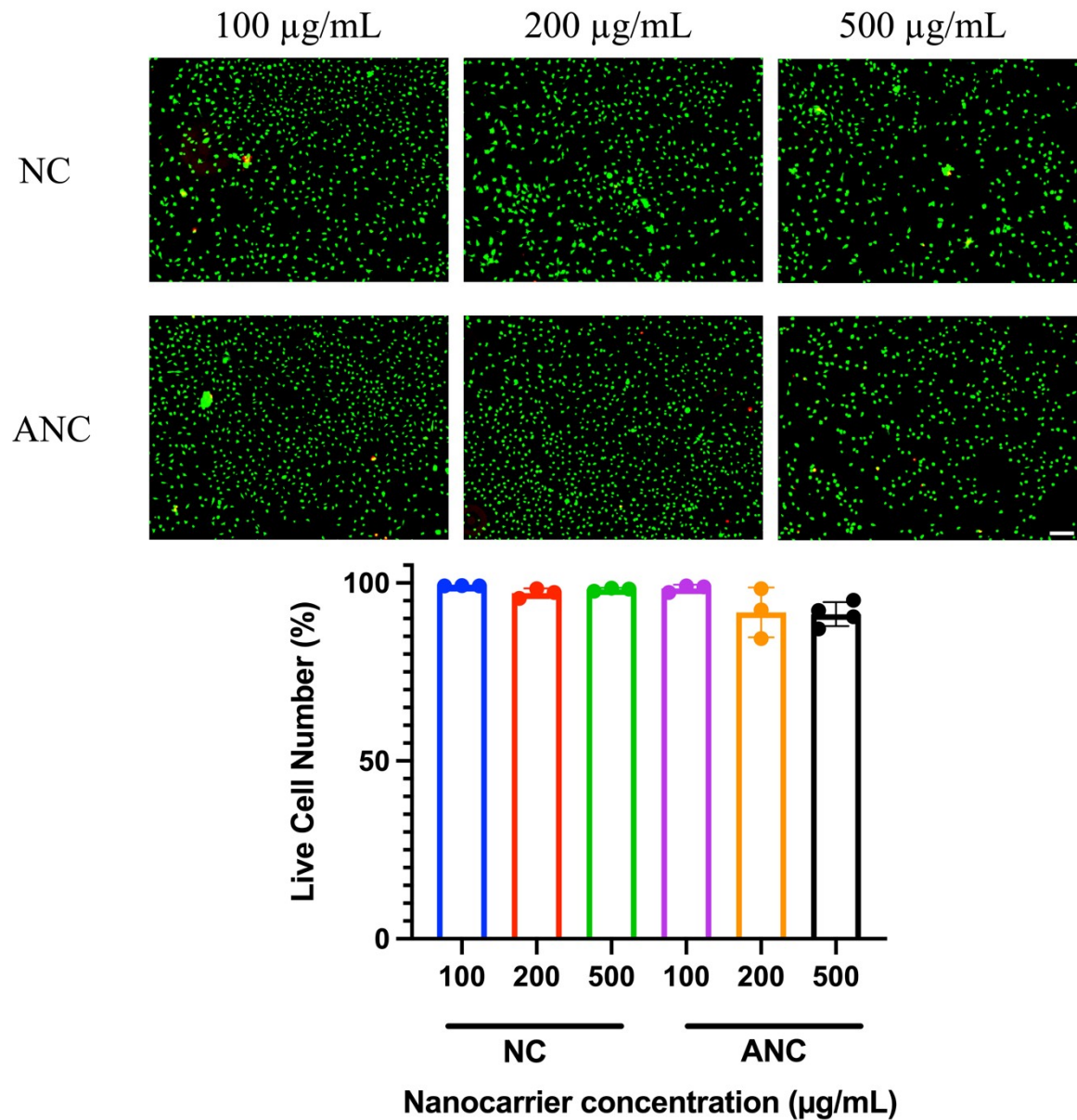


Figure S11. Cytotoxicity of the nanocarriers. (a) Live/dead images of bone marrow mesenchymal stem cells treated with either NC or ANC at various concentrations of 100 µg/mL, 200 µg/mL, and 500 µg/mL for 24 hours. (b) Quantification of the live/dead images. Green: live cells. Red: dead cells. n = 3-4; Scale bar: 50 µm.

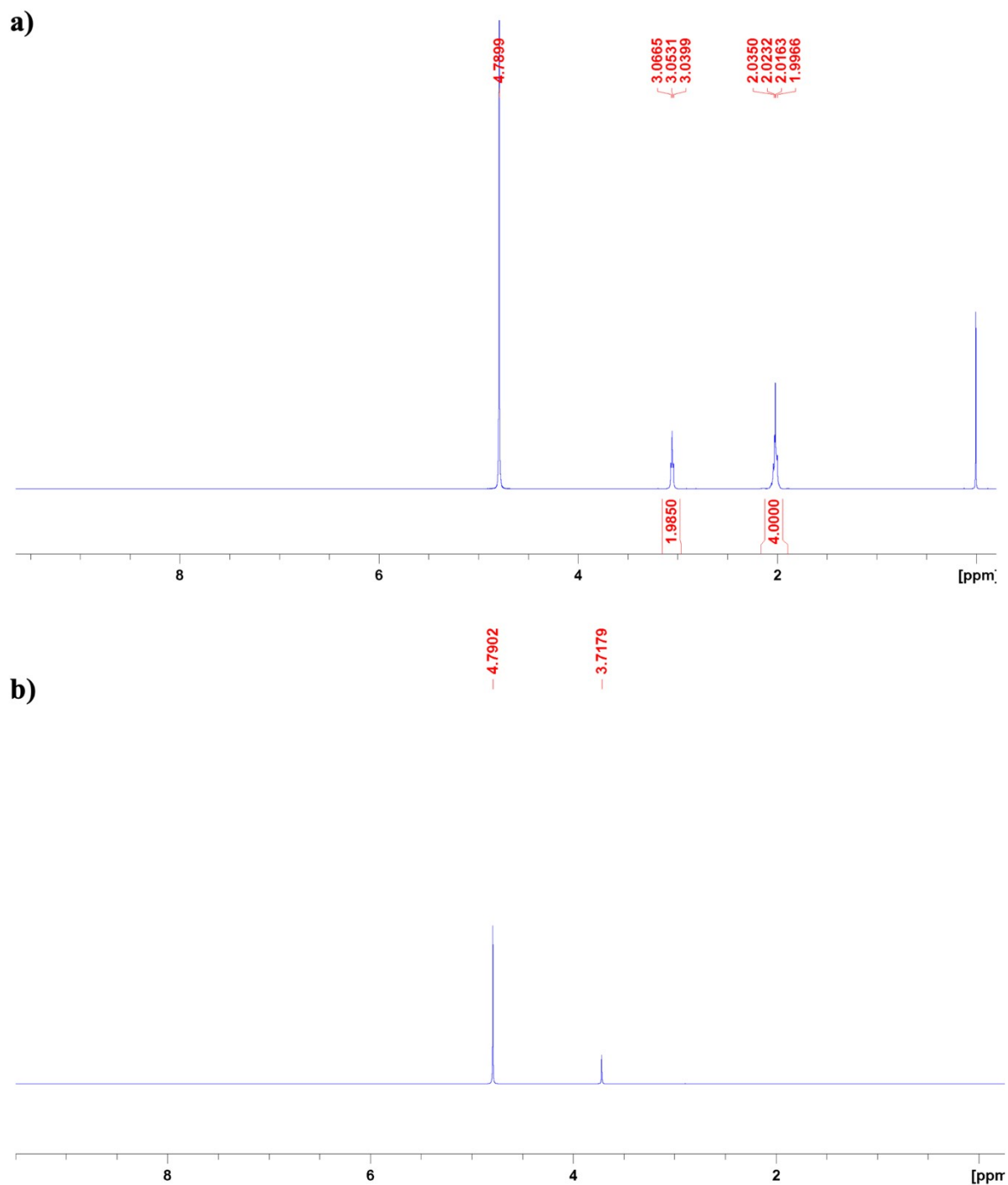


Figure S12. ^1H NMR spectrum of (a) sodium alendronate and (b) freeze-dried residue of the incubating medium. Both the spectra were recorded at 500 MHz in D_2O . No peaks corresponding to methylene protons of alendronate at 2.02 and 3.05 ppm were observed in the freeze-dried product.

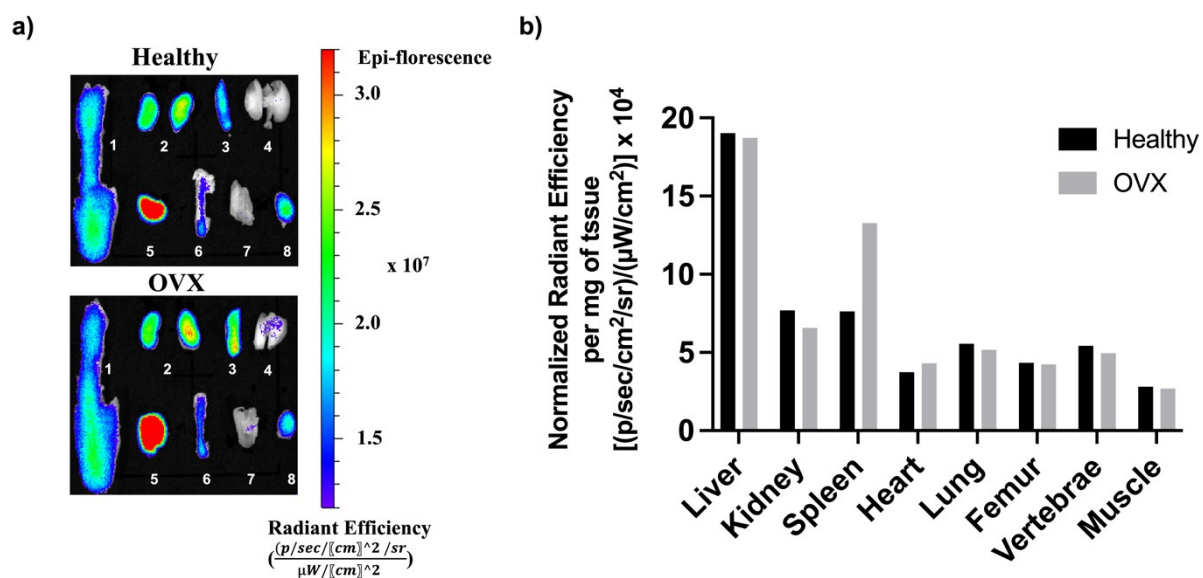


Figure S13. Biodistribution of the adenosine-loaded nanocarrier, ANC. (a) Accumulation of the ANC in major organs of healthy and OVX mice. (b) Radiant efficiency of the fluorescent signal in various organs represented per milligram of the tissue for healthy and OVX mice. In panel (a): 1: Vertebrae, 2: Kidneys, 3: Spleen, 4: Lung, 5: Liver (piece), 6: Femur, 7: Muscle, 8: Heart. n = 4-5.

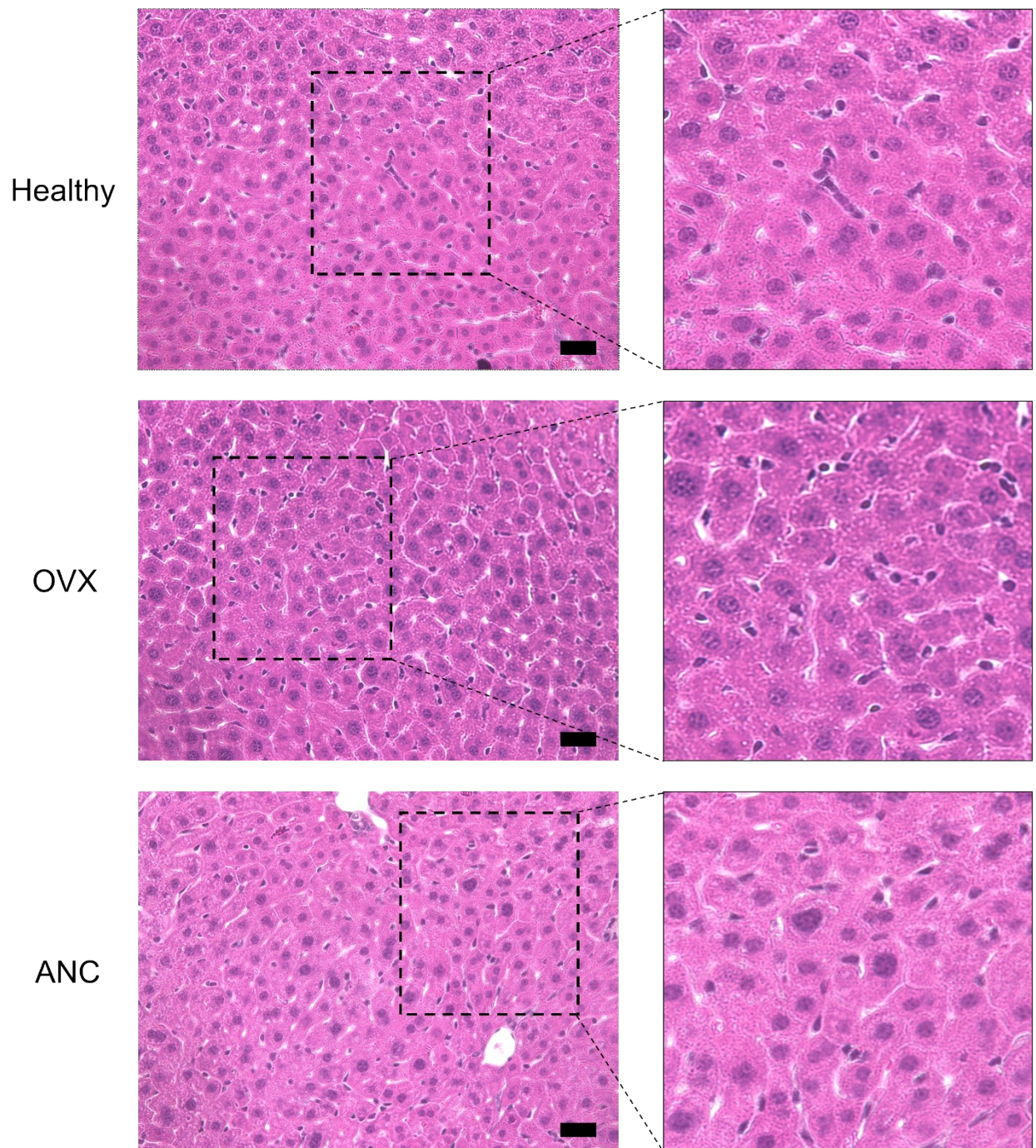


Figure S14. Hematoxylin and eosin staining of the liver following weekly administration of the adenosine-containing nanocarrier (ANC) in OVX mice for 8 weeks. Three different groups were examined: healthy control group without OVX (H), OVX without treatment (O), and OVX treated with adenosine-containing nanocarrier (ANC). $n = 4$ (representative image). Scale bar: 50 μm .

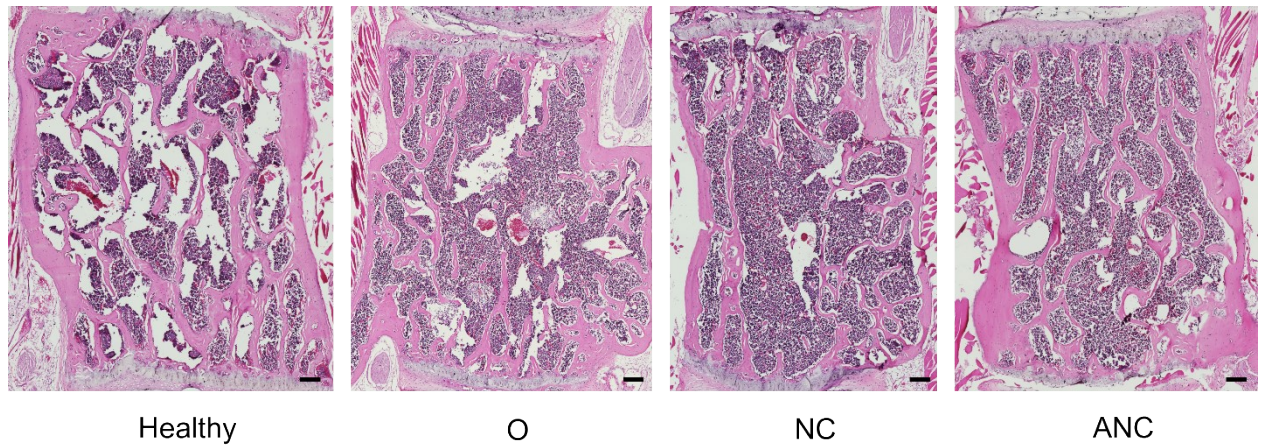


Figure S15. Hematoxylin and eosin staining of the L4 Vertebrae of different animal groups. Weekly administration of the nanocarrier without adenosine (NC) and adenosine containing nanocarrier (ANC) in OVX mice occurred for 8 weeks. Four different groups were used: healthy control group without OVX (H), OVX without treatment (O), OVX treated with nanocarrier only (NC), and OVX treated with adenosine containing nanocarrier (ANC). n = 4-5 (representative image). Scale bar: 100 μ m.

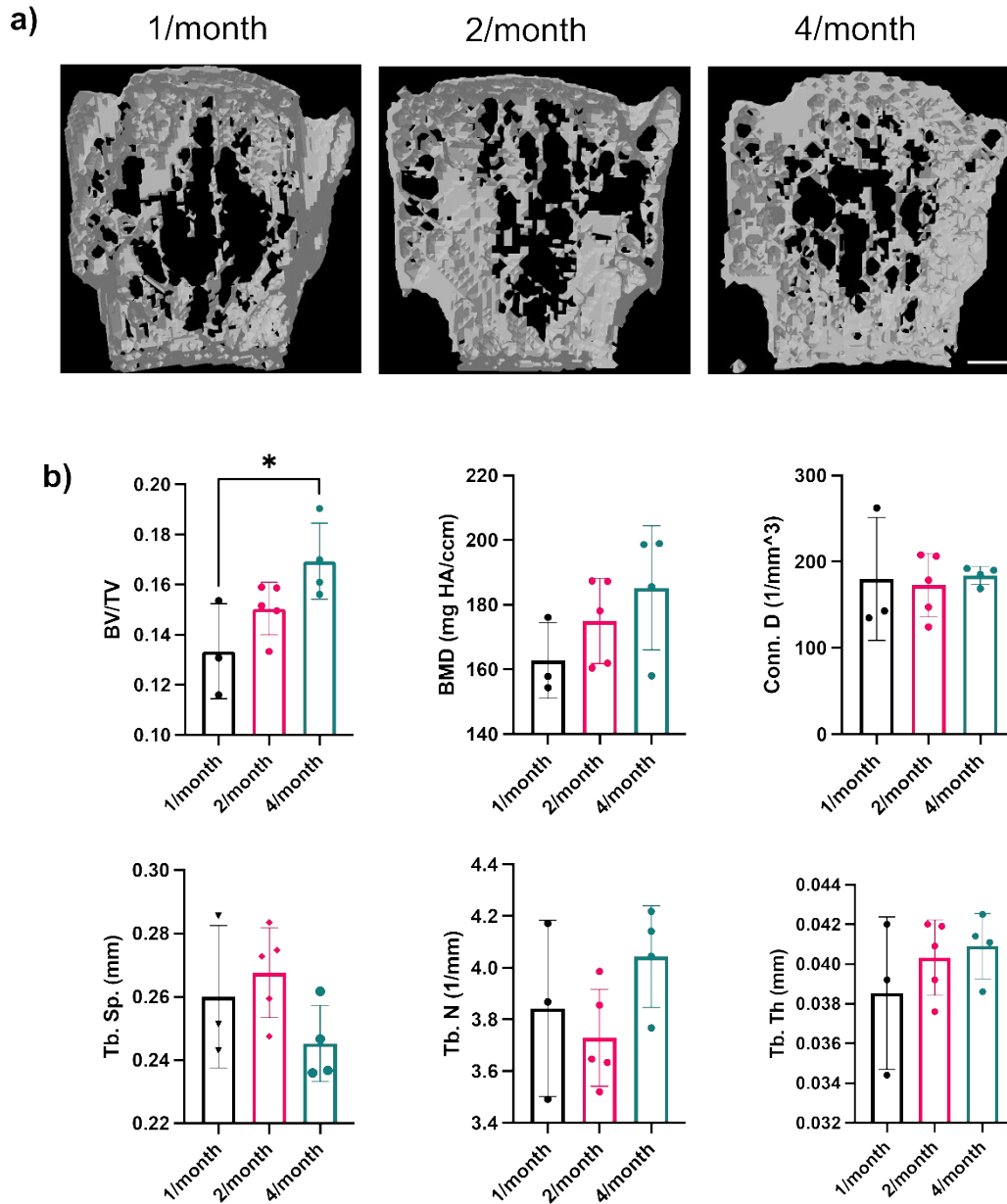


Figure S16. Frequency of ANC administration and its effect on osteoporotic bone loss. Monthly (1/month), biweekly (2/month) and weekly (4/month) administration of the nanocarrier containing adenosine (ANC) for 8 weeks (a) Reconstructed micro-CT images of vertebrae corresponding to different dosing regimen (Scale bar: 500 μ m). (b) Quantification of the micro-CT images: Ration of bone volume (BV/TV); bone mineral density (BMD); connectivity density (Conn. D.); trabecular spacing (Tb.Sp.); trabecular thickness (Tb. Th.); trabecular number (Tb. N.). n = 3-5 per group. *p<0.05.

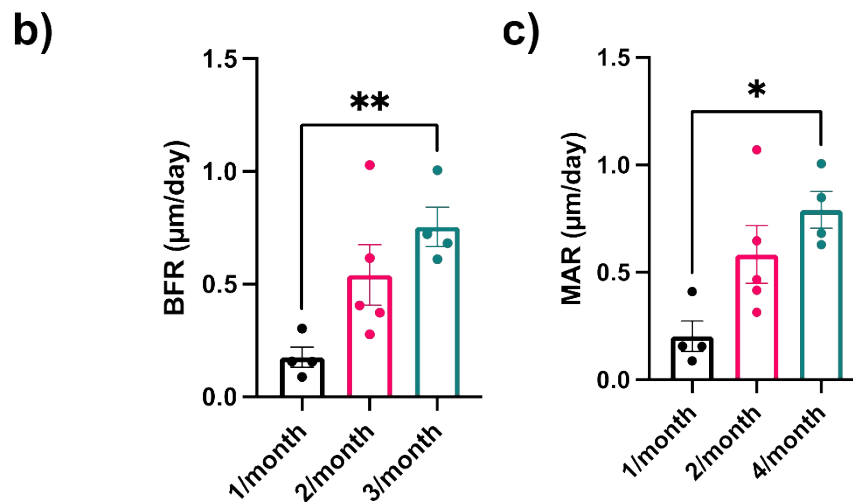
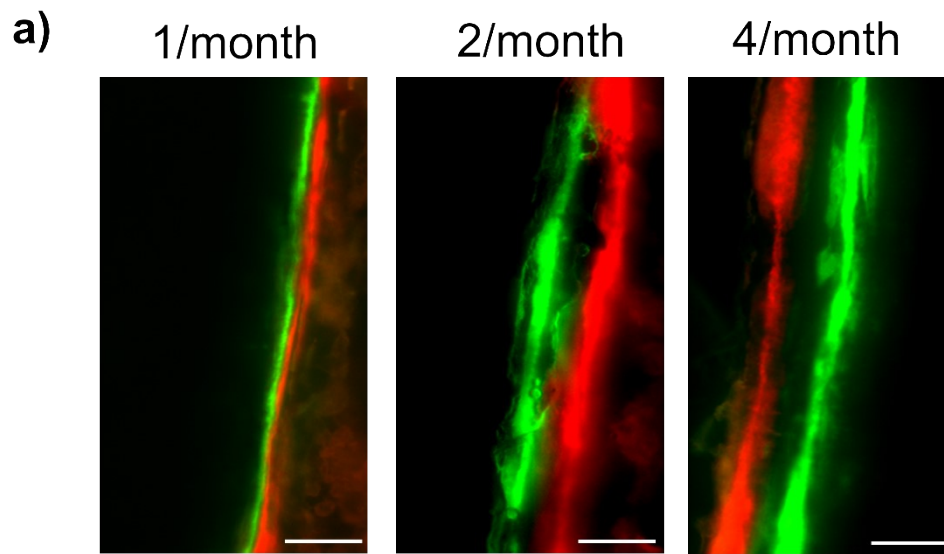


Figure S17. Higher frequency of ANC administration promoted increased new bone formation. Monthly (1/month), biweekly (2/month) and weekly (4/month) administration of the nanocarrier with (ANC) for 8 weeks. (a) Double fluorescence bone labeling by calcein (green) and alizarin complexone (red) of the femur ($n = 3-5$ with representative images, scale bars: $20 \mu\text{m}$). (b) Quantification of bone formation rate (BFR) from bone labeling images. (c) Quantification of mineral apposition rate (MAR) from bone labeling images. * $p < 0.05$, ** $p < 0.01$